ARTICLE NO. 78-1352R

High Performance Dash-on-Warning Air Mobile Missile System

D. S. Hague*
Aerophysics Research Corporation, Bellevue, Wash.
and
Alan D. Levin†
NASA Ames Research Center, Moffett Field, Calif.

On receipt of warning, the air mobile aircraft-missile system performs a high acceleration takeoff followed by a supersonic dash to a "safe" distance from the launch site. At that time a subsonic long endurance mode is entered. The study objectives were to 1) determine technological aircraft and boost trajectory requirements, 2) provide initial definition of the aircraft and boost trajectory requirements, and 3) provide partial cost estimates for a fleet of aircraft which provides 200 missile on airborne alert. Three aircraft boost propulsion systems were studied: an unstaged cryogenic rocket, an unstaged storable liquid, and a solid rocket staged system. Aircraft gross weight was minimized for the combined dash and endurance mission profile. Using existing technologies, the resulting vehicles could accomplish the mission for gross weights of approximately one million lb.

I. Introduction

DURING the past decade land based strategic missile systems have become increasingly vulnerable to attack as ICBM terminal miss distances have been decreased. This factor has prompted a search for mobile systems which would be less vulnerable to a first strike attack.

Dash-on-warning concepts are one of several candidate designs capable of reducing the first strike threat. In this concept, advanced ICBM's are carried within the fuselage of large high performance subsonic-supersonic aircraft. These vehicles are maintained in a ground alert status. On warning of an impeding attack or threat, the aircraft-missile system combination performs a high acceleration take-off and dash to a safe location from the launch site. Following the dash, a subsonic long endurance flight segment is entered to permit assessment of the threat prior to taking appropriate responsive action. These actions may vary from maintaining an air alert status with conventional horizontal landing and take-off refuelling of the carrier aircraft, to the launch of a retaliatory strike, Fig. 1.

This paper deals with the selection of dash trajectories, the impact of dash fuel requirements on system design, and selection of the optimal carrier aircraft design concept.

II. Design Concepts

A matrix of vehicle design concepts was selected for investigation as candidate dash-on-warning configurations, Fig. 2. These configurations fall into three major categories: staged, unstaged, and alternatives. Staged concepts employ vertical take-off and a single solid rocket booster similar to that used on the space shuttle system. Unstaged concepts employ vertical take-off and four internally carried reusable liquid rocket engines using either cryogenic or storable fuels. Alternative concepts investigated included a horizontal take-off design with ten duct-burning afterburning engines employed in the dash. Six of these engines were then turned off in the subsonic loiter mode. This concept was eliminated in early studies as its gross weight was in excess of 2×10^6 lb. A modified space shuttle design was also considered in the vertical take-off mode. This concept could meet the dash segment, but with reduced payload, and hence was deemed unacceptable.

The staged and unstaged systems retained for further study were each subjected to further preliminary design studies using the NASA "Aircraft Synthesis Program, ACSYNT," of Refs. 1 to 4. This code contains preliminary design level analysis modules for all major disciplines entering into the dash-on-warning system design, Fig. 3. The configurations investigated in this manner were designed to three concepts: a two position wing swept back along the fuselage during boost, a conventional variable sweep wing, and finally a fixed wing concept. The nominal payload consisted of two 100,000-lb advanced missiles carried internally; design excursions also considered two or four internally carried 80,000-lb missiles, Fig. 4.

III. Ballistic Dashes

Early sizing studies employed ballistic flight profiles for the dash segment, Fig. 5. Following a maximum thrust vertical ascent to 1000 ft, the optimal pitch over for a zero lift dash to 50 n.mi. in three minutes was determined by multivariable search techniques, Refs. 5 and 6, embodied in Refs. 7 to 10

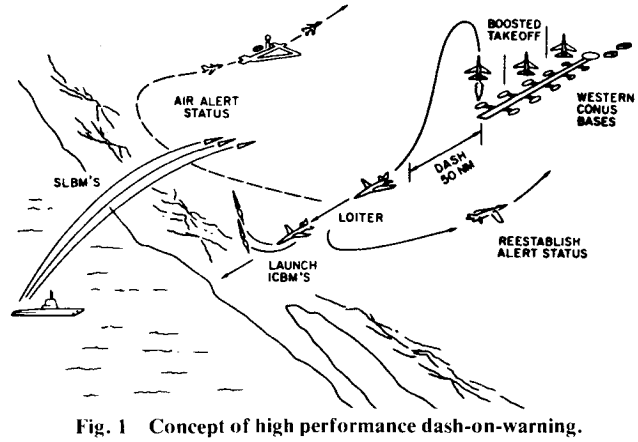

Fig. 1 Concept of high performance dash-on-warning.

Presented as Paper 78-1352 at the AIAA Atmospheric Flight Mechanics Conference, Palo Alto, Calif., Aug. 7-9, 1978; submitted Sept. 11, 1978.

Index categories: LV/M Mission Studies and Economics; LV/M Propulsion and Propellant Systems; Missile Systems.

*President. Member AIAA.

†Research Scientist.

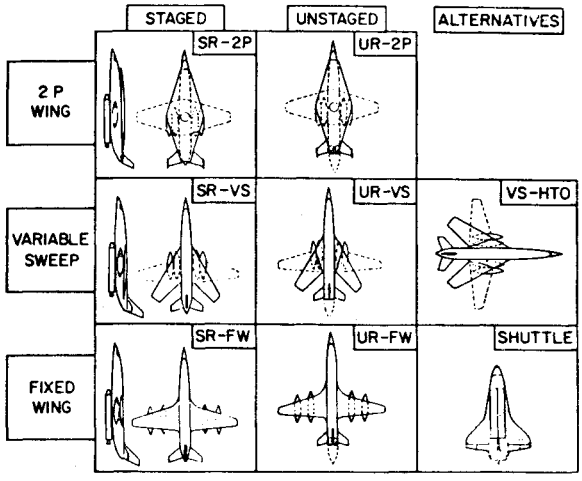

Fig. 2 Matrix of aircraft concepts.

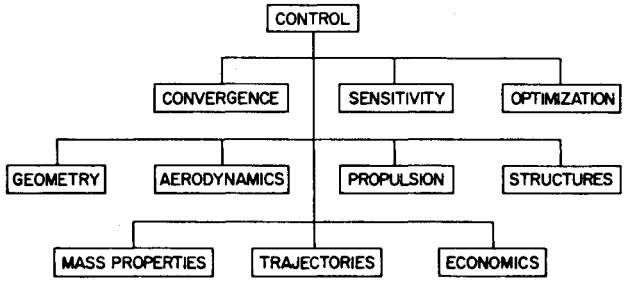

Fig. 3 Synthesis program block diagram.

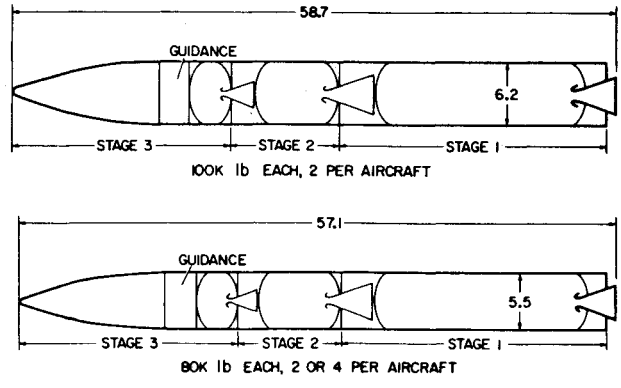

Fig. 4 Missile designs.

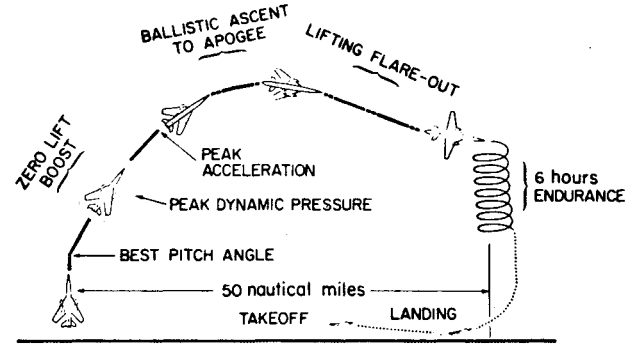

Fig. 5 Ballistic mission profile.

"Atmospheric Trajectory Optimization Program, ATOP." A ballistic path was followed to apogee and a lifting flare out at maximum lift/drag was employed in the descent to the 50 n.mi. point. The aircraft design then permitted six hours subsonic endurance cruise before refuelling. Peak dynamic pressures typically occurred in the mid-region of the boost period. Peak axial accelerations occur immediately prior to boost burnout and, in the final designs discussed below, had values on the order of 3g.

Using this trajectory model, boost fuel fraction as a percent of initial weight was determined as a function of installed thrust weight, with burn times determined to satisfy the dash requirement. Typically, with this dash profile, required thrust/weight for minimum boost fuel fraction was on the order of 3.0. The corresponding boost fuel fraction approached 30%, Fig. 6. Boost fuel fraction was found to be quite sensitive to certain design characteristics. For example, at a given thrust/weight, an aircraft designed with the high body fineness ratios and thin wing thickness-chord ratios required for efficient supersonic flight, required almost 20% less boost fuel than a configuration designed for efficient subsonic flight, Fig. 7. It was apparent from this and other similar results that a design compromise had to be made between dash and endurance portions of the mission. This compromise involved the use of wings somewhat thicker than those normally employed in supersonic flight and body fineness ratios higher than those of conventional subsonic aircraft, Ref. 4. These designs achieved the maximum axial accelerations of about 3g as previously noted.

IV. Effect of Dash Time

The effect of varying dash time to reach 50 n.mi. was briefly studied and the results are shown in Fig. 8. These results were obtained using the modified space shuttle vehicle. Dash times of 2 and 3 min were studied with no constraint on the maximum dynamic pressure. The three-minute dash was achieved at a maximum dynamic pressure of about 1700 psf and required a boost fuel fraction of 54.2% for an initial thrust-to-weight ratio of 2. The two-minute dash required dynamic pressures of about 3000 psf. For a thrust-to-weight ratio of 2, the boost fuel fraction was 69.7%. Increasing the thrust-to-weight ratio to 3 reduced the fuel fraction to 66.3%. Because the dynamic pressure requirements and boost fuel fractions are much larger for the two-minute dash, only the three-minute dash was considered for further investigation.

A typical altitude-range profile for both the two- and three-minute dash is shown in Fig. 9. In this example the three-minute dash requires a burn time of about 76 s; the two-minute dash requires a burn all the way (120 s), and is about 1 n.mi. short of reaching the 50 n.mi. target range. The Mach numbers at the end of the dash were slightly over the 3 for the three-minute dash and nearly 7 for the two-minute dash. The two-minute dash would therefore require aircraft designed for hypersonic flight conditions.

The parametric approach and ballistic ascent indicated that lowering the boost dynamic pressure will rapidly increase the required boost fuel fraction from those shown in Fig. 8. It also became apparent that a lifting, variable-thrust, shaped trajectory would be a better approach to simultaneously control the dynamic pressure and to determine the path that minimizes the boost fuel fraction. The remainder of this paper deals with trajectories and designs employing optimal shaped trajectories.

V. Optimal Variational Trajectories

Time varying optimal control history trajectories were obtained using the variational calculus option of the program cited in Refs. 7 to 10. The mission profile for a typical optimal trajectory is shown in Fig. 10. After a vertical rise of 1000 ft, the vehicle is pitched over to follow a lifting boost path to burnout. The path is determined by varying the throttle setting and angle of attack to remain within specified dynamic pressure constraints. Peak dynamic pressure typically occurs at supersonic speeds beginning about the middle of the burn period, with the maximum acceleration of about 3g's oc-

curring near burnout. The lifting vehicle coasts to apogee at nearly constant energy. A gliding re-entry is performed to keep entry dynamic pressures low. After the gliding re-entry the vehicle geometry is changed near the beginning of the subsonic endurance portion of the mission profile. A subsonic cruise endurance segment is then flown. At the end of the endurance portion of the mission profile, the vehicle has the capability to land, refuel and take off in a horizontal mode under the power of the cruise engines alone.

VI. Flight Profile

An actual optimal Mach-altitude path flow in shown in Fig. 11. The vehicle accelerates at low altitudes and reaches a Mach number of 1 at an altitude of slightly over 20,000 ft. The dynamic pressure placard, in this case 500 psf, is picked up supersonically and followed to burnout. Burnout occurs near a Mach number of 3 and at an altitude of 70,000 ft. The vehicle then follows a nearly constant energy path to an apogee of about 100,000 ft. The 50 n.mi. point is reached at a Mach number of slightly over 2.5 an altitude of about 80,000 ft. A constant dynamic pressure path on the order of 200 to 300 psf is then followed to the best speed and altitude for the endurance portion of the mission profile. For the configurations studied, the best Mach number for endurance flight is 0.55 at an altitude between 22,000 ft and 27,000 ft depending upon the vehicle geometry, mass, and propulsive and aerodynamic characteristics.

Typical dynamic pressure histories for the shaped trajectory with a staged-rocket fixed-wing and an unstaged-rocket two-position wing are shown in Fig. 12. The constraint on maximum boost dynamic pressure is again 500 psf and is imposed by driving the line integral of the dynamic pressure violation to zero by the method of Ref. 7. To minimize the fuel fraction, the vehicle trajectory reaches the dynamic pressure placard quickly and then maintains the placard boundary throughout boost. After burnout, there is a decay in dynamic pressure as the vehicle coasts at nearly constant

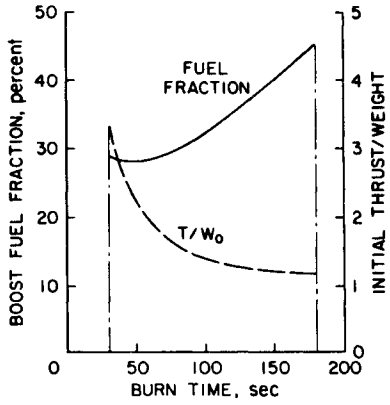

Fig. 6 Boost fuel fraction and thrust-to-weight ratio, ballistic profile, LOX/H_2.

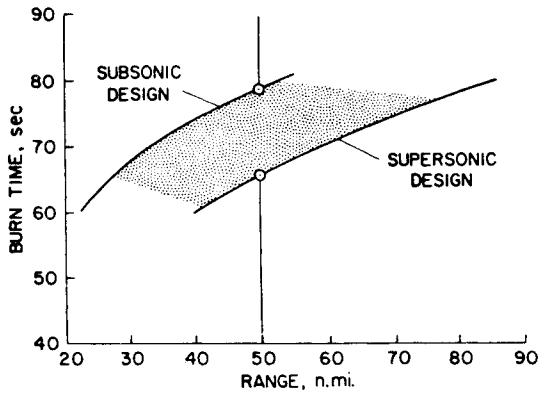

Fig. 7 Effect of aircraft design on boost fuel requirement.

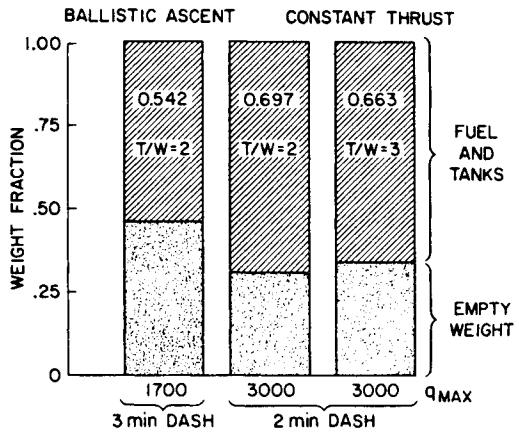

Fig. 8 Effect of dash time on boost fuel fraction.

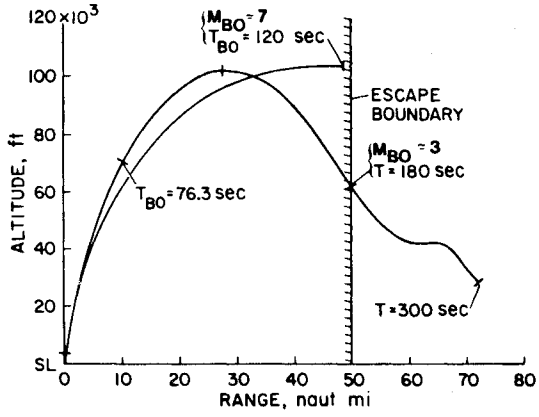

Fig. 9 Typical VTO range-altitude flight profiles.

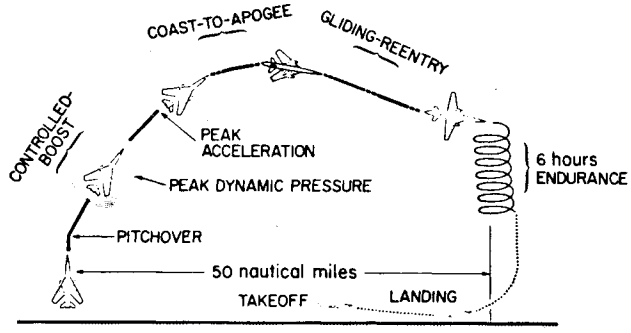

Fig. 10 Throttle and angle-of-attack controlled mission profile.

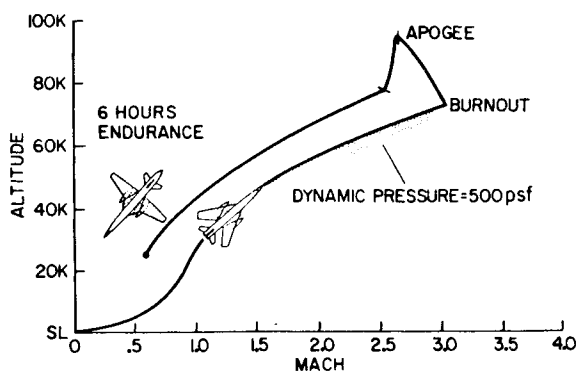

Fig. 11 Typical trajectory, throttle and angle-of-attack profile.

energy to apogee; then a rise in dynamic pressure occurs as re-entry begins. The entry dynamic pressures and those following the descent to the endurance flight conditions have a maximum value of about 60% of the boost dynamic pressure placard level. There is a slight violation of the 500 psf boundary during boost, which could be removed with further shaping. However, the violation is only about 5% greater than the constraint value and does not have a significant effect on either the boost fuel fraction or the vehicle design.

A typical control history of throttle setting and angle-of-attack schedule for the 500 psf dynamic pressure placard are shown in Fig. 13. The history shown is for an unstaged rocket which has a limit on the vacuum thrust of the four shuttle engines of 2.12 million lb. This thrust level constraint is also imposed as a violation integral. There is an initial violation of the thrust level, but the violation shown has little effect on the fuel fraction.

The thrust decays initially as the dynamic pressure placard is reached, and then begins to rise towards the end of the main burn. After termination of the main burn, there is a low level thrust requirement of about 20% thrust from one engine until the end of the three-minute dash. It is assumed that this deep throttle of the boost engines can be achieved by design changes of the present boost propulsion system. The angle-of-attack schedule followed shows variations of about -3 to $+1$ deg angle of attack, until apogee is reached. The 10 deg angle of attack is required during the re-entry to maintain low dynamic pressure.

Physical Basis for Optimal Path

A straightforward explanation of the optimal boost paths obtained in the study is possible. The path which the vehicle must follow is indicated by the optimal boost corridor shown in Fig. 14. The corridor through which the vehicle must fly is shown in the altitude-velocity plane. Minimum velocity at a given altitude during boost is that velocity corresponding to vertical flight. This lower bound is shown for a thrust-to-weight ratio of 1.5. The maximum velocity at a given altitude is defined by the dynamic pressure constraint, in this case 500 psf. Increasing the thrust-to-weight ratio moves the minimum velocity boundary closer to the dynamic pressure boundary and can close the corridor. Similarly, decreasing the dynamic pressure moves the maximum velocity boundary toward the minimum velocity boundary and can also close the corridor. Therefore considerable care must be given to the choice of both the thrust-to-weight ratio and dynamic pressure limits to insure that a corridor remains open along the entire flight profile. The actual variational optimum path followed by the vehicle is indicated on the figure. The vehicle initially remains close to the thrust-to-weight ratio velocity boundary near Mach 1 at an altitude of about 20,000 ft. From that point until burnout, the vehicle maintains a path along the maximum allowable dynamic pressure boundary. Burnout is terminated when the vehicle energy is sufficient to meet the time constraint to reach 50 n.mi. at minimum boost fuel fraction.

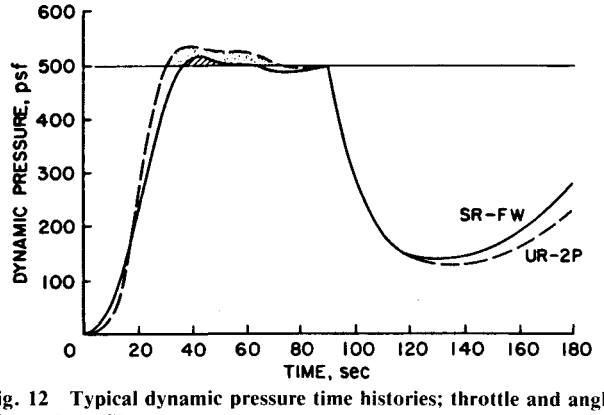

Fig. 12 Typical dynamic pressure time histories; throttle and angle-of-attack profile.

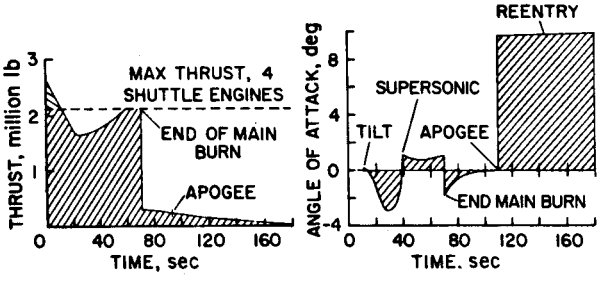

Fig. 13 Typical control histories for throttle and angle-of-attack profile.

VII. Boost Fuel Fraction

The boost fuel fraction as a function of dynamic pressure is shown in Fig. 15. Curves are presented for the staged rocket configuration which used the solid strap-on boost system and the two unstaged rocket configurations, which use either the storable liquid propellant, UDMH, or the cryogenic liquid propellant, LOX/H_2. For the staged rocket configurations, the boost fuel fraction shown includes the casing weight to hold the propellant. Fuel fractions are highest at the lowest dynamic pressure limit. For the fixed wing configurations at a boost dynamic pressure of 500 psf, the staged rocket systems have the highest fuel fraction. This is a result of the lower energy content of the boost propellant. For the staged system, the fraction is about 65% of the vehicle gross weight. For the unstaged rocket, the storable liquid system requires a boost fuel fraction of about 50%. The cryogenic propellant, being the most energetic of those studied, requires a boost fuel

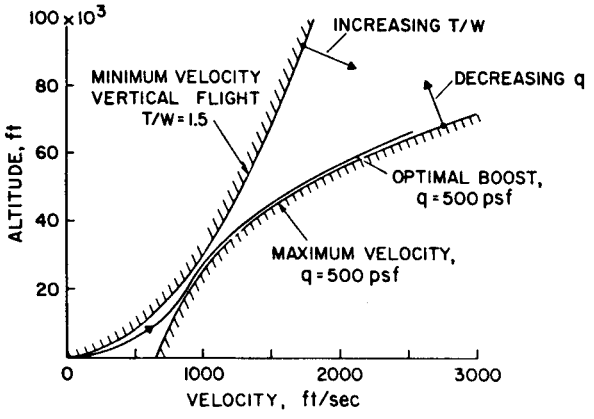

Fig. 14 Optimal boost corridor; dynamic pressure-500 psf.

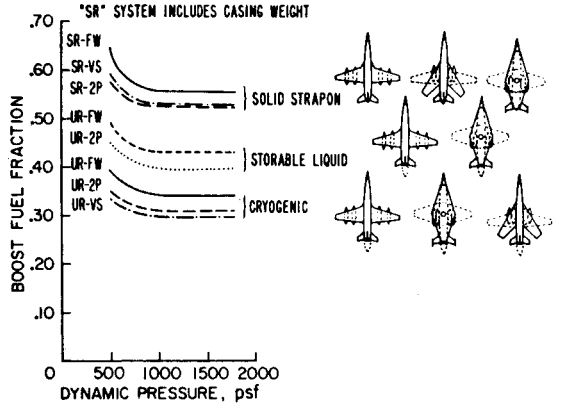

Fig. 15 Variation of boost fuel fraction with boost dynamic pressure.

fraction of about 40%. For the variable geometry configurations, the required boost fuel fraction is less, indicating the more favorable drag characteristics compared to the fixed wing configuration. As the boost dynamic pressure is permitted to increase to about 1000 psf there is a rapid reduction in the boost fuel requirement. For dynamic pressures greater than 1000 psf, there is only a slight further reduction in the boost fuel fraction.

VIII. Dynamic Pressure Effect on Structure

As indicated in Fig. 15, higher dynamic pressure decreases the boost fuel fraction. However boost fuel is only one aspect of the problem. The effect of dynamic pressure on the vehicle structural weight must also be taken into account. As the boost dynamic pressure is increased, the vehicle structure becomes heavier. This tradeoff between design dynamic pressure and gross weight is illustrated in Fig. 16. Results are presented for the unstaged rocket using cryogenic propellant. The trends for the other rocket systems are similar.

The design dynamic pressure has a margin of 40% over the boost dynamic pressure. Therefore a design dynamic pressure of 700 psf is required for a boost dynamic pressure of 500 psf. For reference purposes the 700 psf design dynamic pressure is typical of current jet transports; 1100 psf represents a value for fighter aircraft such as the F-5A; and the F111 has been designed for a dynamic pressure of about 2000 psf.

The variable sweep aircraft is the lightest vehicle at the lowest dynamic pressure, but becomes the heaviest vehicle at the maximum pressure of 1300 psf considered. The fixed-wing aircraft is somewhat heavier than the variable sweep aircraft at the nominal design dynamic pressure and does not rise as rapidly as the variable-sweep wing aircraft. Conversely, the two-position wing indicates a reverse trend with increasing dynamic pressure. This configuration is the heaviest at the lowest design dynamic pressure and becomes lighter with increasing dynamic pressure. This converse behavior is due to the wing being aligned with the fuselage during boost and attached rigidly to the fuselage near the wing tips. Therefore, it is not subjected to high dynamic pressure loads during the boost portion of the flight. There is a slight increase in the weight of the tails and flight controls with increasing dynamic pressure, but the wing is a larger fraction of the airframe weight.

It should be noted that the curves of Fig. 16 represent vehicles which have been optimized for each dynamic pressure and therefore are not the same vehicle operated at different dynamic pressures. The lower weight vehicles have a relatively high aspect ratio wing; those vehicles designed for the highest dynamic pressures have a low aspect ratio wing. This is true for both the fixed-wing and variable-sweep wing aircraft. For the two-position wing, the aspect ratio remains the same since it is aligned with the fuselage and requires no design changes to withstand the higher boost dynamic pressures.

IX. Economics

The nominal requirement for the economic study was to maintain 200 missiles airborne during an attack. For an assumed launch probability of 90%, the purchase of a fleet of 112 aircraft is required to satisfy dash-on-warning system requirements. Partial cost elements used in this study were development and acquisition costs to purchase the fleet and fuel costs for 10 years of operation as a function of the number of fleet launches. An aggregate learning curve of 80% was used on acquisition costs, comparable to current experience trends in the aerospace industry. In particular, this learning rate is typical of that encountered in the design of subsonic jet transport aircraft. It has been shown that the empty weights of dash-on-warning aircraft are comparable to current big subsonic jets and they employ similar airframe and cruise engine technology.

In addition to airframe costs, the additional costs associated with boost propulsion acquisition are considered.

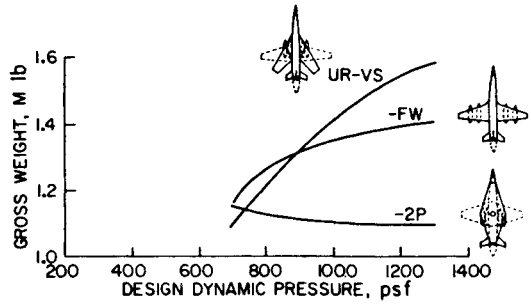

Fig 16 Variation of gross weight with design dynamic pressure.

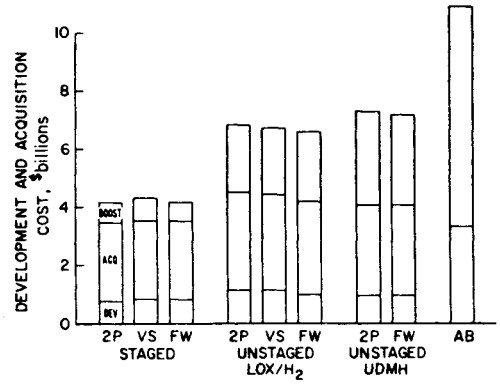

Fig. 17 Development and acquisition cost comparison; 200 missiles airborne, 112 aircraft.

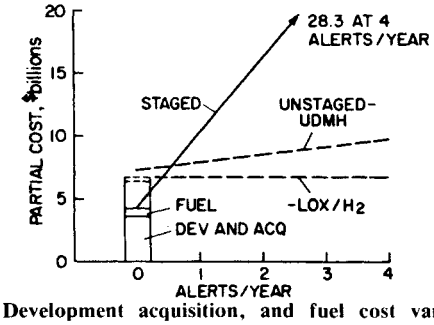

Fig. 18 Development acquisition, and fuel cost variation with number of fleet alerts; 10 years, 6 h/alert, 200 missiles airborne.

For the solid rocket booster, this cost was $6 million per launch per aircraft. The booster was considered expendable; although the space shuttle booster is recoverable, for its launches are preplanned rather than forced by a potential attack.

The cost of the space shuttle cryogenic rocket engine is estimated to be $5 million each. Four rocket engines are required for the unstaged rocket systems, resulting in a boost propulsion cost of $20 million per aircraft. This is a nonrecurring cost since these reusable engines remain with the vehicle throughout the entire mission profile. The UDMH rocket engines are about the same size and thrust class as the cryogenic engines. Therefore, it was assumed they would also cost $20 million per aircraft. In addition to the acquisition cost, the UDMH engine would require a development cost of approximately $800 million which was the estimated development cost of the shuttle engine. If this cost is amortized over 112 operational aircraft, the total cost of UDMH boost engines is $27 million per aircraft, $7 million more per aircraft than the cryogenic rocket engines. The cruise engine cost is estimated to be $1 million per engine, the current acquisition cost for CF-6, JT-9, or TF-39 engines which power the DC-10, 747, and C-5A, respectively.

Fuel costs used in this study were $0.2 per pound for LOX and $.50/lb for H_2. For the mixture ratios of LOX to H_2, this

results in a net price of $.10/lb for the propellant combination. The cost for the storable propellant components was $.14/lb for nitrogen tetroxide, $.50/lb for UDMH, and $4/lb for hydrazine. For the fuel-to-oxidizer ratios required, the combined propellant cost is $1/lb. The cruise engine JP-4 fuel cost was $.30/gal. The cost of solid propellant fuel for the staged rocket is included in the $6 million acquisition cost.

A comparison of the development and acquisition cost, in billions of dollars, for the various concepts is shown in Fig. 17. Development, acquisition, and initial boost system costs are presented. Independent of wing geometry, the staged rocket development and acquisition cost is about $4 billion. The unstaged cryogenic concepts have higher development and acquisition costs, primarily reflecting their heavier empty weights. The initial cost of the unstaged rocket boost system is also larger than the staged rocket concept. Again, independent of wing geometry, cryogenic unstaged rocket development and acquisition cost are about $7 billion. The storable liquid propellant concept are somewhat more costly than the cryogenic concepts. This primarily reflects the development cost of a new UDMH rocket engine. The all air-breathing HTO concept was the most costly, with a partial cost of about $11 billion. This reflects the heavy empty weight of the aircraft and the development and acquisition costs associated with advanced airbreathing engines in the 200,000-lb thrust class. The costs shown for the variable geometry configurations did not consider the increased complexity due to wing pivots.

A complete economic analysis of the system including maintenance and operational costs lay outside the present study scope. However, a partial cost estimate covering development acquisition, and fuel costs is possible. Fig. 18 shows the partial cost as a function of alerts (or training flights) per year. Partial cost is defined here as development and acquisition costs for the fleet and fuel costs for 10 years. The aircraft are assumed to be airborne 6 hours per alert. Four alerts per year represent a total of 40 fleet alerts over the 10 years. Only the fixed-wing configurations are presented, but they require the greatest boost propellant due to their higher configuration drag.

From an initial cost of $4 billion the staged rocket costs rise rapidly with number of alerts per year. Each fleet alert requires the purchase of a new $6 million booster for each aircraft. The net boost cost per alert is $600 million for replacement of the expendable solid rocket. At four alerts per year, the partial cost for staged rocket system is about $28 billion. The cryogenic unstaged rocket is initially more costly than a staged rocket, but even at four alerts per year there is only a slight rise in cost. The only costs which accrue to this system at each launch are boost and cruise fuels, since the rocket engines and tanks are reusable. At four alerts per year, the unstaged rocket UMDH cost is about $3 billion more than the cryogenic. This reflects the higher cost of the UDMH propellant.

X. Concluding Remarks

All the new concepts studied satisfied the mission profile of a 50 n.mi. dash in 3 min, 6-hour endurance, and 200,000 lb of payload. One of the most significant findings is that the supersonic dash can be achieved at a dynamic pressure of 500 psf. This is about the same dynamic pressure encountered by current subsonic jet transports and suggests that conventional large subsonic jet structure and material technology can be used for the airframe. The airframe can be made from conventional aluminum structure, and the cruise engines used for endurance flight are in operation today. Either the CF-6 or JT-9 will satisfy the endurance cruise and conventional takeoff and landing requirements. The cryogenic unstaged rocket concepts utilize the current space shuttle rocket engine design. Costs are quoted in 1974 dollars.

All the candidate configurations weighed more than one million lb at launch. There is a negligible weight difference among the three wing geometries considered and between the cryogenic and storable liquid boost propellants. At launch, unstaged rockets are about 20% lighter than staged rockets because they use a more energetic boost propellant. Conversely, during endurance flight, the staged rockets are about 40% lighter than unstaged rockets because they have no dead weight associated with the boost. The empty weight and endurance flight weight are similar to the big subsonic jet transports.

The development, acquisition, and boost propulsion costs to maintain 200 missiles on air alert for six hours will be about $4 billion for staged rockets and about $7 billion for unstaged rockets. Staged rocket costs are highly sensitive to the number of alerts or training flights per year because they require an expendable booster. The cost will be nearly $600 million for each fleet alert. Therefore, the unstaged rockets appear to be the lowest cost configuration if even a few fleet training flights or alerts are planned. For these aircraft, the boost propulsion system is reusable, and therefore only fuel costs are incurred at each alert.

One final point should be made regarding the philosophy of the system. It is apparent that the dash-on-warning concept is basically a defensive rather than offensive system. It can be launched on warning rather than on attack and offers the time for a considered response in a given situation. It is equally clear that offensive systems can be designed far more easily than the concepts discussed in this paper.

References

[1] Gregory, T.J., "Computerized Preliminary Design at the Early Stages of Vehicle Definition," Presented at AGARD Flight Mechanics Panel Meeting on Aircraft Design Integration Optimization, Florence, Italy, Oct. 1-4, 1973.

[2] Nelms, W.P. and Axelson, J.A., "Preliminary Performance Estimates of a Highly Maneuverable Remotely Piloted Vehicle," NASA TN D-7551, 1974.

[3] Nelms, W.P., Murphy, R. and Barlow, A., "Preliminary Analysis of Long Range Aircraft Designs for Future Heavy Airlift Missions," NASA TM X-73131, June 1976.

[4] Levin, A.D., Castellano, C.R., and Hague, D.S., "High Performance Dash-on-Warning Air Mobile System," NASA TM X-62479.

[5] Hague, D.S. and Glatt, C.R., "An Introduction to Multivariable Search Techniques for Parameter Optimization, "NASA CR-73200, April 1968.

[6] Hague, D.S. and Glatt, C.R., "A Guide to the Automated Engineering and Scientific Optimization Program—AESOP," NASA CR-73201, June 1968.

[7] Hague, D.S., "Three-Degree-of-Freedom Problem Optimization Formulation," FDL-TDR-64-1, Part I, Volume III, 1964.

[8] Hague, D.S., "Atmospheric and Near Planet Trajectory Optimization by the Variational Steepest-Descent Method," NASA CR-73365, Aug. 1968.

[9] Hague, D.S., "Application of the Variational Steepest-Descent Method to High Performance Aircraft Trajectory Optimization," NASA CR-73366, 1969.

[10] Hague, D.S., "The Optimization of Multiple Arc Trajectories by the Steepest-Descent Method," *Recent Advances in Optimization Techniques,* edited by Lavi and Vogl, Wiley, N.Y., 1969, pp. 489-517.